Outcomes of multifarious selection on the evolution of visual signals

Justin Yeager[1†*] and Olivier Penacchio[2,3†]

[1] Biodiversidad Medio Ambiente y Salud, Universidad de Las Américas, 170125 Quito, Ecuador.

[2] School of Psychology and Neuroscience, University of St Andrews, St Andrews, Fife KY16 9JP, United Kingdom

[3] Computer Vision Center, Computer Science Department, Universitat Autònoma de Barcelona, Bellaterra, 08193 Barcelona, Spain

[†] Authors contributed equally

* Corresponding author; e-mail: yeagerjd@gmail.com

Abstract:
Multifarious sources of selection shape visual signals and can produce phenotypic divergence. Theory predicts that variance in warning signals should be minimal due to purifying selection, yet polymorphism is abundant. While in some instances divergent signals can evolve into discrete morphs, continuously variable phenotypes are also encountered in natural populations. Notwithstanding, we currently have an incomplete understanding of how combinations of selection shape fitness landscapes, particularly those which produce polymorphism. We modeled how combinations of natural and sexual selection act on aposematic traits within a single population to gain insights into what combinations of selection favors the evolution and maintenance of phenotypic variation. With a rich foundation of studies on selection and phenotypic divergence, we reference the poison frog genus *Oophaga* to model signal evolution. Multifarious selection on aposematic traits created the topology of our model's fitness landscape by approximating different scenarios found in natural populations. Combined, the model produced all types of phenotypic variation found in frog populations, namely monomorphism, continuous variation, and discrete polymorphism. Our results afford advances into how multifarious selection shapes phenotypic divergence, which, along with additional modelling enhancements, will allow us to further our understanding of visual signal evolution.

Introduction

Animal visual signals are readily measurable quantitative traits which facilitate intra- and interspecific communication, whose divergence can be used to measure the influence of diverse sources of selection. Aposematic coloration is a specific class of visual signal, which advertises unprofitability of prey to potential predators [1]. Aposematic signals often vary geographically, with locally-adapted phenotypes evolving in response to different combinations of selection pressures. [2]. Selection often produces a single dominant phenotype in a given area and time (monomorphism), which may differ between geographic regions (polytypism). However, in some instances multiple divergent forms co-occur geographically (polymorphism). The evolution and maintenance of polymorphism has been a long-standing puzzle, yet polymorphism has been found with increasing frequency, even in aposematic species [3]. However, we currently lack detailed understanding of how sources of selection interact to shape the evolution of visual signals under multifarious selection, and specifically under what conditions polymorphism arise.

Various combinations of both natural and sexual selection can permit, or even promote polymorphism [4-8], even within aposematic species. In addition to defensive functions evolved under natural selection, the conspicuous nature of aposematic signals makes them ideal traits to be co-opted by sexual selection. In poison frogs for example aposematic signals are used in mate choice [9-11], as well as male-male conflict where they may vary and correspond with dominance [4, 12] or other behavioral traits like boldness [13]. In these species there are multiple potential ways in which multifarious selection can operate simultaneously, such as working either synergistically or in opposition [14], on single or multiple traits of visual signals. Ultimately the specific combination of multiple sources of selection will determine whether divergence is promoted or suppressed. Interacting sources of selection and geographic isolation between divergent aposematic signals can thus create different fitness landscapes, where locally adapted aposematic color patterns occupy peaks of the local fitness landscape, and transition regions are thought to be occupied by valleys. Our understanding of the evolutionary formation, maintenance and trajectory of signal divergence is contingent on our ability to predict how these sources of selection influence traits.

As cases of polymorphism are found with increasing frequency, it remains unclear which, and how, sources of multifarious selection have produced and maintained observed levels of warning color diversity in aposematic species. Stable polymorphism could evolve and be maintained by various balances of selection. Alternatively, if polymorphism is transient, divergent phenotypes could be lost (reverting to monomorphism); or conversely, color polymorphism could be enhanced and contribute to reproductive isolation and potentially speciation [15]. Empirical studies of natural populations can provide valuable insights into the influence of different types of natural and sexual selection on warning signals. Similarly, they can demonstrate how relaxed selection, or the absence of one source of selection, could produce polymorphism through neutral processes such as drift [16]. However, being limited to these contemporary snapshots, we are often left with an incomplete understanding of how selection shaped the early stages of phenotypically divergent populations. Moreover, we do not know which selection regimes render polymorphism a stable state, or if they are more likely to

instead transition and enhance divergence towards speciation or rather diminish due to admixture or hybridization. Mathematical models can be leveraged to better analyze phenotypic evolution in evolutionary timescales and enhance our understanding of evolutionary processes (e.g. [17]), but have only been applied as simple qualitative models for polymorphism [18-20].

Here we characterize alternative evolutionary outcomes for phenotypic divergence resulting from diverse combinations of selection pressures acting synergistically (with both equal, and differing intensities) on aposematic signal traits. To leverage empirical examples, the different forms of our model are loosely based on studies in the poison frog genus *Oophaga*. This group of frogs is ideal to model as the majority of *Oophaga* species are polytypic, displaying geographic variation in color patterns [21-24], and there are additionally many instances of within-population polymorphic populations [21, 24-26]. There is also specific evidence that multifarious selection has shaped phenotypes [27]. Aposematic coloration has been affirmed to deter predators [28], therefore demonstrating a selective pressure on warning signals through predation. However, predation risk, even phenotype-specific, varies across a phenotypic radiation [29-32]. Among members of the genus *Oophaga*, evidence is mixed for local avoidance being higher for local phenotypes [29, 31, 33] and generalized avoidance is even suggested [23]. Therefore, although evidence of varying strengths of natural selection via predation is found, predation may contemporaneously be shaping phenotypic divergence less than sexual selection. Evidence of sexual selection can be found in terms of assortative mate choice [9, 34, 35], though in some instances a single morph is preferred [4, 6, 11].

We propose a simplified quantitative model to estimate the influence of two distinct sources of selection (here we refer to as natural and sexual, but they could just as well be multiple sources of natural or sexual selection) on the evolution and stability of two quantitative traits of aposematic signals. The permutations of our model aim to better understand phenotypic evolution by measuring the influence of diverse parameters; differences in how selection acts on visual signals traits (e.g., chromatic versus luminance contrast) by implementing different intensities of selection. Specifically, our models aim to disentangle which combination(s) result in different evolutionary outcomes such as stable polymorphism (continuous or discrete), versus those which collapse into monomorphism. Model outcomes represent predictions of the distributions of phenotypes related to their evolution under multifarious selection. These predictions can be subsequently evaluated in empirical studies to infer whether the type and degree of signal variance reflects the combinations of selection strengths at play.

Methods

Model Outline

We model how two sources of selection create a fitness landscape, and therefore influence and shape the evolution of a population's distribution of phenotypes, such as aposematic signals in poison frogs. Our aim was to go beyond contemporary snapshots that empirical studies have afforded to estimate evolutionary outcomes of multifarious selection. Importantly, we also aimed to model the evolution of the whole distribution of phenotypes in a population, not only of its mean and standard deviation [36], as it would otherwise be impossible to monitor polymorphic outcomes. We considered the distribution of phenotypes of a population. Possible phenotypes

formed a two-dimensional continuous space (x, y) in $[0, 1] \times [0, 1]$, where x and y were abstract variables describing two traits such as, for example, luminance contrast and chromatic contrast (see Figure 1 for definitions and illustration corresponding to this example). Over evolutionary timescales, starting from a minimally variable population, phenotypes evolved continuously subject to both random mutations and selective forces. The heritability of the phenotypes was reflected by these continuous changes (i.e., the distribution of phenotypes at one time step was close to the distribution at the next time step). To model random mutations, the phenotypes inherited from one generation to the next were subject to random variations (Brownian motion), which permitted us to model fine-scale divergence in phenotypic signals. We assumed that sexual reproduction generated a constant level of random variations in the next generation phenotype, which was modeled using a diffusion process in which diffusion was uniform (i.e., did not depend on the location (x, y) in the phenotypic space) and isotropic (did not depend on the direction in the phenotypic space). We focused on a simplified model which does not take into account any type of frequency dependent selection, and considered a population with a constant number of individuals (see Supplementary Materials). To model the effect of selection, we supposed that each phenotype was subject to three types of evolutionary forces, sexual selection, natural selection, and the cost of signal production and maintenance, each leading to a specific fitness surface, namely W_{sex} for sexual selection, W_{nat} for natural selection, and W_{cost} for signaling cost. Taken together, these fitness surfaces formed an adaptive landscape, i.e., a landscape that associated an average fitness to each phenotype [37] as

$$W_{total} = W_{sex} + W_{nat} + W_{cost}. \qquad (1)$$

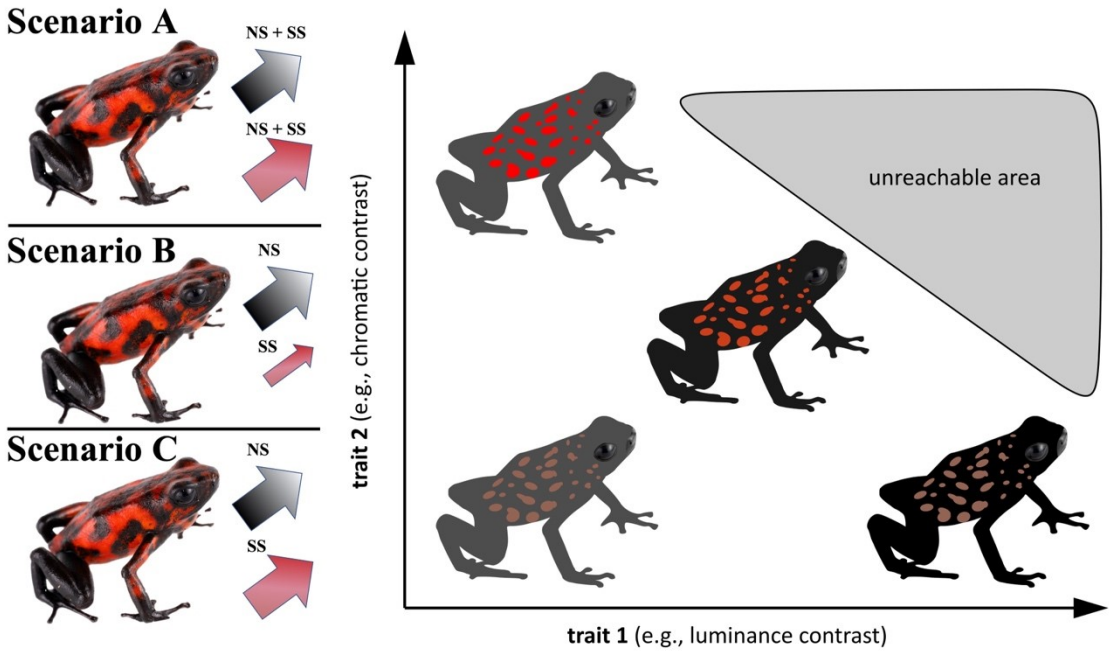

Figure 1. We model three different scenarios for how two sources of selection (shown here as Natural Selection, NS, and Sexual Selection, SS) act on two phenotypic quantitative traits: luminance contrast (black/white arrow) and chromatic contrast (red arrow). Luminance contrast is provided by differences in intensity, but not in spectral composition, of signal elements, and is processed by achromatic channels (in birds for example it is measured by differences in the responses of double cones). Chromatic contrast refers to differences in spectral composition but not intensity, and is driven by chromatic mechanisms (e.g., differences between the responses of long-, medium-, short- and ultraviolet wavelength sensitive cones in birds) [38]. Scenario A demonstrates both NS and SS acting with equivalent strengths on both luminance and chromatic contrast. Scenarios B and C show NS and SS acting on different traits, but at different strengths (SS weak in Scenario B, and equal strengths in Scenario C). The right-hand portion of the figure shows the potential evolutionary outcomes for aposematic signals by increasing luminance contrast, chromatic contrast, or both. The gray shaded region indicates phenotypic combinations that are unattainable due to the physical impossibility to generate a visual signal with both maximum luminance and chromatic contrast. Here, for example, it is impossible for the two reflectance values that determine luminance and chromatic contrast to maximally

differ in intensity (while having the same chromatic spectrum) and maximally differ in spectral composition (while having the same achromatic intensity, see Supplementary S2 for more details). Photos courtesy of J. Culebras.

While the evolution of each individuals' phenotype is stochastic due to the random diffusion component, the evolution of the population's distribution of phenotypes can be fully described using the deterministic Fokker-Planck equation. The distribution that maximizes fitness on the fitness landscape W_{total} is the unique stationary solution of the Fokker-Plank equation

$$\frac{\partial \rho}{\partial t} = \mathrm{div}(\nabla \Psi(x,y)\rho) + D\Delta\rho, \tag{2}$$

where ρ is the probability density function of the population phenotypes, which gives the probability of phenotype (x, y) at time t as $\rho(x, y, t)$, D is the (constant) diffusion term, and Ψ is a function on the phenotypic space related to the fitness landscape W_{total}. More precisely, the distribution $\hat{\rho}$ that maximizes fitness is the distribution that minimizes the free energy

$$F_E(\rho) = \int_{[0,1]^2} \Psi(x,y)\rho(x,y,t)\,dx\,dy + D\int_{[0,1]^2} \rho(x,y,t)\log(\rho(x,y,t))\,dx\,dy, \tag{3}$$

with

$$\Psi(x,y) = -W_{\mathrm{total}}(x,y), \tag{4}$$

and can be computed as the unique stationary solution of Equation (2) [39, 40]. Note that with the minus sign in Equation (4), minimizing the free energy F_E amounts to maximizing the fitness of the population phenotypes on the fitness landscape W_{total}. We modeled the evolution of phenotypes from a starting distribution $\rho_0 = \rho(x, y, 0)$ until convergence to the distribution with maximal fitness $\hat{\rho} = \rho(x, y, \infty)$ in different evolutionary scenarios (cf. below for details on the computations). Phenotypes evolve continuously over evolutionary time in step-wise fashions from the previous generation (traits are therefore heritable) subject to random forces from mutations and evolutionary forces in accordance with the fitness landscapes created by sources of selection. We highlight that our model differs from others in that we track continuous evolution of phenotypic divergence at the level of the whole population rather than population averages [36]. Using tools from statistical physics such as the Fokker-Plank equation was therefore critical as the mean and standard deviation of the distribution of phenotypes would not be sufficient to distinguish monomorphism from continuous or discrete polymorphism. While we assume phenotypic traits are heritable, we track the evolution of traits themselves, rather than the genetic underpinnings that result in their expression, as this permits us to include diverse color pattern elements which influence predation risk [28] taking into account environmental contributions such as dietary carotenoids or alkaloids (e.g., [41]; see Supplementary Materials for further general modeling details).

Different evolutionary scenarios

To illustrate the effect that different combinations of selective forces can have on the evolutionary outcome of a population, we considered three distinct scenarios where selection acted equally on both traits, with different intensities on different traits, and with the same intensity on different traits. In all scenarios, diffusion, namely the random variations of phenotypes from one generation to the next, was the same (and constant across the phenotypic space). This reflects

the neutral assumption that mutations occur at the same rate everywhere in the phenotypic space. Enhancing the strength of the signal traits is unlikely to occur without a cost (especially in honest signals [42]), therefore a cost function was included, which was the same across scenarios, and associated a high cost to high values of both traits. In the exemplified version of the model in which traits 1 and 2 correspond to luminance and chromatic contrast, a high value for both traits were impossible due to the physical impossibility to maximize luminance and chromatic contrast simultaneously (see Supplementary Materials S2). Accordingly, only the forces of natural and sexual selection differed between scenarios. Our model is inspired by, and loosely based on, the evolution of visual aposematic signals in *Oophaga* poison frogs, where color patterns are under both natural and sexual selection. In light of the weight of empirical studies, we chose to focus our model on scenarios in which selection acts either synergistically, or in parallel (acting on alternate traits) on these aposematic signals, rather than in opposition or antagonistically. Within- and between differences have been quantified in coloration including chromatic and luminance contrast (see Figure 2B from [10]) which can be influenced by multifarious selection, potentially due to different combinations of natural and sexual selection on visual signals (see Supplementary Materials for further details).

In scenario A, the forces of natural and sexual selection were mainly compatible, both favoring equally higher values for both traits, as shown by the similarity between the landscapes W_{sex} and W_{nat}, Figure 2, scenario A. This scenario represents a population in which both predators and sources of sexual selection favor overall highly contrasting conspicuous aposematic signals. In scenarios B and C, natural and sexual selection exerted different pressures on the two phenotypic traits, where natural selection in this model favors higher values for trait 1 and sexual selection higher values for trait 2, reflected by the 'orthogonality' between the landscapes W_{sex} and W_{nat}, Figure 2, scenario B and C. Both scenarios were different, however, in the sense that in scenario B one of the forces (W_{sex}) had a lower magnitude than the other (W_{nat}), whereas both were of the same magnitude in Scenario C. Scenario B creates an example in which natural predator exert stronger selection over trait 1 (e.g., luminance contrast) than sexual selection for trait 2 (e.g., chromatic contrast). However, in Scenario C the strength of selection exerted is equivalent between sources of selection, but predation's pressure favors enhanced luminance contrast, whereas conspecifics favor enhanced chromatic contrast. This resulted in different fitness landscapes W_{total}. In scenario A, given the high cost of having high values for both aposematic traits, this led to an adaptive landscape with a wide peak, or ridge of constant height, as shown in W_{total}, Figure 2, scenario A. All individual phenotypes in the landscape were expected to climb towards this ridge. We refer to the set of starting points in the phenotypic space as a "basin" from which phenotypes tend to leave by climbing toward a given peak or ridge of constant height (optima). In scenario A the initial position of the population within the phenotypic space is within this single basin where optima were characterized by a long crest rather than a single peak. In scenario B, there was a single optimum ('peak') in the landscape. Accordingly, there was a single basin in the landscape, and all phenotypes were expected to climb towards this peak, Figure 2, scenario B. In scenario C, by contrast, there were two optima, which defined two basins, i.e., the fitness landscape W_{total} could be partitioned into two areas defined by the peak a phenotype was expected to climb towards, Figure 2, scenario C. These scenarios were the selection-influenced landscapes under which we modeled the population-wide evolution of frog phenotypes to assess their evolutionary outcomes, producing such outcomes as monomorphism or continuous or discrete polymorphism.

Model implementation

The Fokker-Planck equation (Equation 2) was solved numerically using code adapted from [43, 44] following a discrete implementation scheme of advection-diffusion equations [45]. The phenotypic space $[0,1] \times [0,1]$ was discretized using $N \times N$ bins of size $1/N \times 1/N$, with $N = 50$. The constant diffusion on the phenotype space was $D = 1/75$. This value was chosen for mutation and selection to cause dynamics with commensurate speeds, but the outcome of the scenarios does not depend on a specific value. To model the cost landscape, we used a sum of power functions. This allowed us to model a slightly increasing cost for increasing values of the traits and prohibitively high costs for very high values of both traits, reflecting the physical impossibility for a signal of having simultaneously a maximal luminance and chromatic contrast (see Supplementary Materials). For modeling the forces of natural and sexual selection we used two-dimensional log functions with a steep increase for low values of the traits, a moderate increase for medium values and a plateauing for higher values. This allowed us to model a general feature in cognition and perception, known as Weber's law, whereby the effect on an increase in a stimulus feature (visual contrast, loudness etc.) is not based on the absolute amplitude of this increase but rather on its amplitude relative to that of the starting stimulus [46]. Accordingly, an increase in amplitude of, for example, 0.1 for a trait of value 0.1 has more effect on a predator (and hence a bigger increase for W_{nat}) or conspecific (hence, a bigger increase for W_{sex}) perception than the same increase for a starting trait of value 0.8. In the numerical simulations we considered 1000 time steps as beyond that point we did not find much evolution on the population's distribution of phenotypes. All the MATLAB [47] and Python [48] functions, and actual values for W_{cost}, W_{nat} and W_{sex}, used for the numerical simulations and generating the figures and videos can be found on the following open-source repository: https://github.com/openacchio/polymorphism-scenarios-and-free-energy-solver. The code and parameters can be directly adapted to draw predictions on the outcome of multifarious selection in other scenarios, including the ability to add more than two sources of selection.

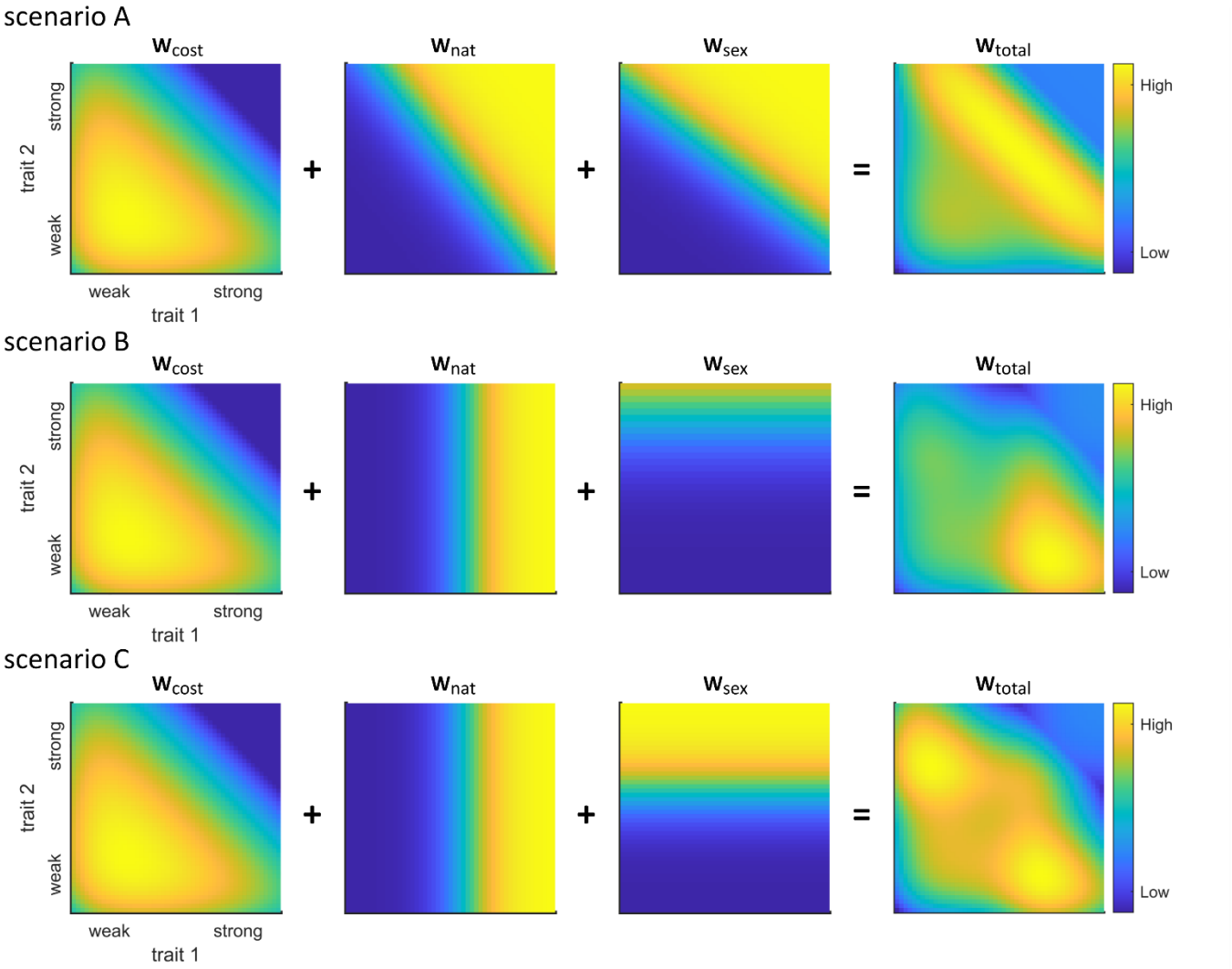

Figure 2. Illustration of the three evolutionary scenarios used for the simulations. In each plot, yellow indicates a high value and dark blue a low value. The fitness landscape, which gives the average fitness for each phenotype in the phenotypic space, results from the interaction between three components, namely fitness related the cost of each phenotype (left panel in each row), to the forces of natural selection (second panel), and to the forces of sexual selection (third panels). The resulting fitness landscape is the sum of these three fitness components (right panel). The cost of the phenotypes was the same across all the scenarios, with high values for both traits associated with a high cost. This allowed us to model both the cost of signal production and the physical impossibility for pattern to 'maximize' both traits (e.g., having maximal luminance contrast and maximal color contrast). In scenario A, the forces of natural and sexual selection were mainly compatible, i.e., of comparable magnitude and both favoring the same phenotypes. In scenario B, the forces were less compatible, natural selection favored high values of trait 1 (e.g., high luminance contrast) independently of trait 2, while sexual selection favored high values of trait 2 (e.g., chromatic contrast) independently of trait 1. In addition, the magnitude of the forces of sexual selection was weaker than the magnitude of natural selection. In scenario C, the forces were similar to those in scenario B, i.e., favoring one trait over the other, but were both strong and of equal magnitude.

Results

Different evolutionary outcomes for scenarios A, B and C are illustrated visually (Figure 3). For each scenario, the left plot shows the population's starting position in the space of phenotypes, superimposed on the total fitness landscape (Figure 2). The middle plot shows populations after 500 evolutionary time steps, whereas the right plot shows the final population (1000 time steps). In scenario A, the final distribution shows that a broad range of phenotypes coexist in the population, where some are more biased towards higher trait 1 values, whereas others evolved towards high values of trait 2. This coexistence, or 'continuous polymorphism', is made possible by the fact that all these phenotypes have comparatively equivalent fitness. In Scenario B, the population converges towards the only fitness peak in the landscape, which illustrates the evolution towards a 'monomorphic' population. When the combination of directions and strengths of selective forces give rise to a more structured fitness landscape, such as those containing two possible optima (Scenario C), the evolutionary outcome for a population depends on the starting location of the population in the space of phenotypes. If the initial phenotypic distribution overlaps the two 'basins' within the fitness landscape (Figure 3, scenario C, case 1), then distribution splits and both parts converge towards distinct phenotypes corresponding to the two different peaks in the two separate basins of the fitness landscape, giving a case of 'true polymorphism'. If the starting distribution lies within one of the two basins, it converges towards a monomorphic distribution of phenotypes with maximal fitness within that basin (Figure 3, scenario C, case 2). The full evolutionary trajectory of each scenario can be seen in the Supplementary Material (scenario A, Suppl. Video 1; scenario B, Suppl. Video 2; scenario C, case 1, Suppl. Video 3, and scenario C, case 2, Suppl. Video 4).

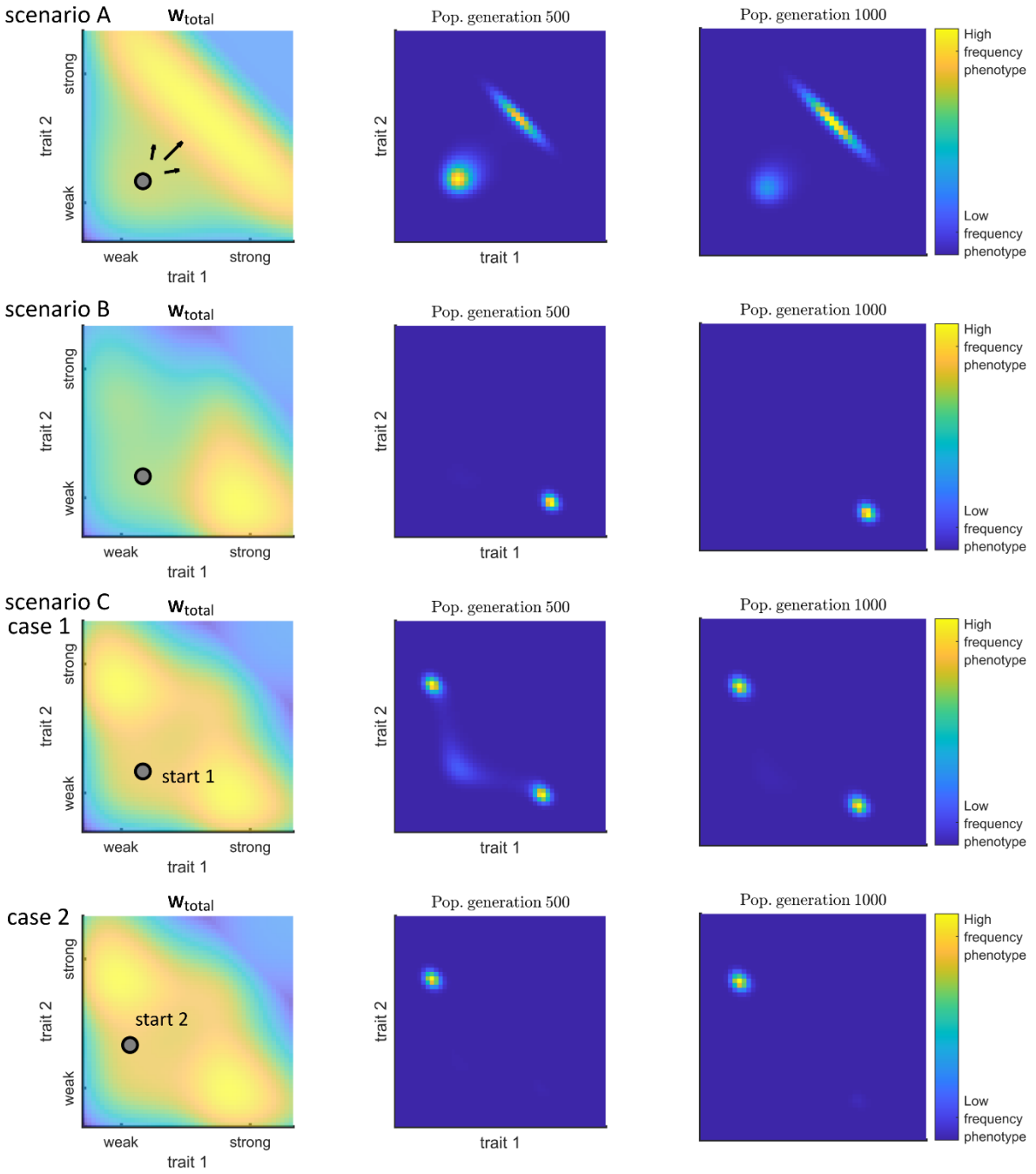

Figure 3. Time evolution of the population's distribution of phenotypes in scenarios A, B and C. For each scenario the distribution of phenotypes in the starting population is shown on the top of the fitness landscape (left column). The middle and right panels show the distribution of phenotypes for generations 500 and 1000 respectively. Scenario A leads to a broad continuous range of phenotypes corresponding to continuous variation in morphs. Scenario B gives rise to a single (monomorphic) phenotype. Scenario C gives two discrete morphs (scenario C, case 1) or a single morph (scenario C, case 2) depending on the location of the original distribution in the phenotypic space.

Discussion

We assessed the potential evolutionary outcomes arising from different combinations of natural and sexual selection acting on elements of a population's aposematic signal. Results from modeling different scenarios indicate that diverse evolutionary outcomes are influenced by both the specific combination of selection (each relative intensities), and whether multifarious

selection acted on the same trait. Starting with a single, variable population, the outcomes produced by different combinations of selection resulted in all types of phenotypic divergence which has been characterized in wild frog populations, including monomorphism [21], continuously variable polymorphism [49], and discrete polymorphism [6].

In our model, the *a priori* chosen combinations of selective forces on visual signaling traits created the fitness landscape topology which, coupled with a Brownian movement/drift element over time, shaped populations traits. When multifarious selection favors a single trait within all possible warning signal combinations (e.g., both natural and sexual selection favor chromatic contrast), continuous phenotypic variation was produced. Interestingly, convergence onto a single optimum (monomorphic phenotype) was produced by natural and sexual selection acting on different traits of the signal (e.g., luminance vs. chromatic contrast), *and* with differing strengths of selection. However, when strong selection acted on different aspects of the aposematic signal, two potential outcomes were possible. Discrete polymorphism was one product, though the population's starting position within a given fitness landscape ultimately dictated whether polymorphism was produced, versus collapsing into a single (monomorphic) phenotype. If the population's initial position placed it closer to a fitness peak for one aspect of the aposematic signal, that trait quickly approached that peak. However, if the initial population started at a location overlapping the border between two fitness basins, then natural and sexual selection could pull the initial population into a discrete polymorphic state favoring alternate traits of the signal.

The topography of a warning signal's fitness landscape can be influenced by a number of combinations of strengths of natural and sexual selection acting on the signals. Understanding the products of interacting sources of selection, as we model with different strengths, is a topic of continued interest [50]. Selection sources in our model largely favored similar conditions, that is optimizing phenotypic trait(s) (chromatic or luminance contrasts in our examples). They differed principally in whether they worked synergistically (e.g., operating on the same trait) or in parallel where each source influenced opposing traits [14].

As aposematic signals tend to favor more conspicuous signals (but see [51]), we did not model where sources of selection could act in opposition. There are countless instances where natural selection could act against, and subsequently suppress traits favored by sexual selection (e.g., [4, 52]). Similarly, inter- or intrasexual conflict could act in opposition on the same, or different traits. A growing literature has taught us that the interests of males and females are not always aligned, and in some extremes can even result in conflict [53]. However, even within a single source of selection, such as sexual selection, the strength of one selection source can overpower a second. For example, female mating preferences for color in *O. pumilio* are superseded by the females preference for the winner of male-male combat, where females choose the territory-holding male even if his color is the less desirable morph [54]. Therefore, it becomes increasingly important to understand the nuances of how diverse sources of selection interact. Empirical studies could lend further support, validating for our model outcomes. Behavioral studies for example could be leveraged to identify key sources of selection and the expression of traits they favor. The fitness-influencing intensities of each type of selection could

be scaled and compared, and the within-population variance in phenotypic traits quantified. The stability of traits could then be measured across generations to infer the stability of phenotypic divergence. Of course, these studies would have challenges and limitations.

Although we discuss these models based on inspiration from populations of the poison frog genus *Oophaga*, for which there is evidence of multifarious selection acting on warning coloration, these results are more broadly applicable beyond the specific details which we described in our model, as there are innumerable scenarios which would result in differences in the composition of sources, and strength of selection. For example, whereas we used natural and sexual selection, we could instead have included two or more sources of sexual selection arising from mate choice and/or intrasexual conflict. Similarly, there could be multiple sources of natural selection, such as instances where color patterns could serve both as a warning signal to predators as well as a role in thermoregulation [55, 56]. Additionally, chromatic and luminance contrasts could easily be substituted for any number of salient quantitative traits that are under selection.

We also acknowledge there are additional important examples of phenotypic variation which our model don't address specifically, such as sexual dimorphism which is indeed found widely ([57], including in poison frogs [58]), and is produced by sources of sexual selection [59]. We would benefit from future studies that specifically explore the population-wide outcomes of different combinations of sex-specific selection. Here we assume that visual signals remain constant as they are in *Oophaga* species, but in other species these signals can be dynamic due to a number of conditions such as hormones or to thermoregulate [60-62]. We reiterate that our model does not feature frequency dependent selection (positive or negative). This limitation means that our model may not be able to track the initial evolution of aposematism, and/or may not properly estimate phenotypic divergence when carried out by part of the distribution of phenotypes separating from the main population. Here we consider that the starting population display aposematic phenotypes, and that the modification of the distribution of phenotypes is slow enough for predators to be able to generalize avoidance towards new phenotypes. Continued efforts should seek to integrate frequency dependence selection to assess its role in multifarious selection.

Our model also assumes that any variation present within populations is salient, and therefore able to be influenced by both natural, and sexual selection. We considered certain aspects of perception of the receiver of the visual signals (predators, conspecifics) by taking into account that animals' sensory perception and subsequent cognitive decisions follow the Weber's law, i.e., are generally based on proportional and not absolute differences [46]. Future models could incorporate more specific inputs related to the visual capabilities of biologically relevant viewers which would describe whether variance reaches detectable threshold, and is salient or not, by the viewers that represent sources of natural and/or sexual selection. For instance, Crothers et al. [63] showed brighter focal males (increased achromatic contrast) solicited more agonistic behaviors from other males, and especially by bright males. However, this variation, which is salient to conspecifics and some predators, is not detectable by all putative major sources of predation [12].

Sensory ecology as a field aims to explore how, and with what precision species acquire and process information within their local habitats, and how that information mediates behaviors. The importance of sensory ecology in studies of speciation has become increasingly clear, as it describes mechanisms which have important implications in how both natural and sexual selection (and their interactions) influence populations at all points along the speciation continuum. Predator perception of warning signals has been incorporated thoroughly in an attempt to explain 'imperfect mimicry'- where the mimic's fidelity to a model species is variable or less ideal [64, 65]. Therefore, the addition of thresholds which reflect the visual capabilities that underlie different sources of selection would add relevant sophistication to our model. For example, different sources of selection may perceive variance in signals before an alternative, and hence influence signal evolution in isolation until the variance becomes salient to the second source.

Our results indicate population-wide phenotypic divergence occurs as little as 500 evolutionary stages (~generations), suggesting that phenotypic shifts can occur relatively rapidly, especially in species with short generation times. One recent study has shown strong selection can also rapidly change visual signals. In *Papilio* butterflies the appearance of a new model species has resulted in enhanced mimetic similarity in a little as dozens of years [66].

The evolutionary trajectory of aposematic populations where warning coloration contains information that is used by sources of natural and sexual selection remains a topic of fervent interest. We have shown just how these sources of selection function in concert, and that whether they influence the same, or differing but related traits, is key to shaping the fitness landscape and ultimately the evolutionary trajectory of aposematic signals. This in turn determines whether these signals ultimately show little variation (monomorphism), or significant variance which produces downstream outcomes such as continuous or discrete polymorphic populations. How different sources of selection combine will ultimately influence whether variation is likely to persist, or even accrue towards speciation, or whether this variation is more likely to be lost and consolidated into a single signal. Empirical studies can continue to inform and refine models such as our to more accurately predict how diverse combinations of interacting multifarious selection influence populations, both for aposematic species and more generally.

Acknowledgments: We thank J. Barnett and B. McEwen for thoughtful comments on a previous daft of this work and J. Culebras for photos in Figure 1. We also thank the associate editor and two anonymous reviewers for thoughtful and constructive feedback. JY received funding support from UDLA internal grant FGE.JY.22.01. OP was funded by the Maria Zambrano grant for attraction of international talent for the requalification of the Spanish university system—NextGeneration EU (ALRC). We also thank participants from the ESEB meeting of multiple predator defenses 2021 for insightful dialogues on prey defenses and predator/prey dynamics which inspired this work.

References

1. Poulton E.B. 1890 *The Colours of Animals: their meaning and use especially considered in the case of Insects*, New York : D. Appleton and Company; 365 p.
2. Chouteau M., Angers B. 2011 The Role of Predators in Maintaining the Geographic Organization of Aposematic Signals. *American Naturalist* **178**(6), 810-817. (doi:10.1086/662667).
3. Briolat E.S., Burdfield-Steel E.R., Paul S.C., Ronka K.H., Seymoure B.M., Stankowich T., Stuckert A.M.M. 2019 Diversity in warning coloration: selective paradox or the norm? *Biological Reviews* **94**(2), 388-414. (doi:10.1111/brv.12460).
4. Rojas B., Burdfield-Steel E., De Pasqual C., Gordon S., Hernandez L., Mappes J., Nokelainen O., Ronka K., Lindstedt C. 2018 Multimodal Aposematic Signals and Their Emerging Role in Mate Attraction. *Frontiers in Ecology and Evolution* **6**, 24. (doi:10.3389/fevo.2018.00093).
5. Finkbeiner S.D., Briscoe A.D., Reed R.D. 2014 Warning signals are seductive: Relative contributions of color and pattern to predator avoidance and mate attraction in Heliconius butterflies. *Evolution* **68**(12), 3410-3420. (doi:10.1111/evo.12524).
6. Yang Y.S., Richards-Zawacki C.L., Devar A., Dugas M.B. 2016 Poison frog color morphs express assortative mate preferences in allopatry but not sympatry. *Evolution* **70**(12), 2778-2788. (doi:10.1111/evo.13079).
7. McLean C.A., Stuart-Fox D. 2014 Geographic variation in animal colour polymorphisms and its role in speciation. *Biological Reviews* **89**(4), 860-873. (doi:10.1111/brv.12083).
8. Hausmann A.E., Freire M., Alfthan S.A., Kuo C.-Y., Linares M., McMillan O., Pardo-Diaz C., Salazar C., Merrill R.M. 2022 Does sexual conflict contribute to the evolution of novel warning patterns? (
9. Maan M.E., Cummings M.E. 2008 Female preferences for aposematic signal components in a polymorphic poison frog. *Evolution* **62**(9), 2334-2345. (doi:10.1111/j.1558-5646.2008.00454.x).
10. Maan M.E., Cummings M.E. 2009 Sexual dimorphism and directional sexual selection on aposematic signals in a poison frog. *Proc Natl Acad Sci U S A* **106**(45), 19072-19077. (doi:10.1073/pnas.0903327106).
11. Richards-Zawacki C.L., Cummings M.E. 2011 Intraspecific reproductive character displacement in a polymorphic poison dart frog, dendrobates pumilio. *Evolution* **65**(1), 259-267. (doi:10.1111/j.1558-5646.2010.01124.x).
12. Crothers L.R., Cummings M.E. 2013 Warning Signal Brightness Variation: Sexual Selection May Work under the Radar of Natural Selection in Populations of a Polytypic Poison Frog. *American Naturalist* **181**(5), E116-E124. (doi:10.1086/670010).
13. Rudh A., Breed M.F., Qvarnstrom A. 2013 Does aggression and explorative behaviour decrease with lost warning coloration? *Biological Journal of the Linnean Society* **108**(1), 116-126. (doi:10.1111/j.1095-8312.2012.02006.x).
14. Allen W.L., Arbuckle K., Aubier T.G., Briolat E.S., Burdfield-Steel E.R., Cheney K.L., Daňková K., Elias M., Hämäläinen L., Herberstein M.E., et al. 2023 The evolution and ecology of multiple antipredator defences. *in revision*.
15. Gray S.M., McKinnon J.S. 2007 Linking color polymorphism maintenance and speciation. *Trends Ecol Evol* **22**(2), 71-79. (doi:10.1016/j.tree.2006.10.005).
16. Runemark A., Hansson B., Pafilis P., Valakos E.D., Svensson E.I. 2010 Island biology and morphological divergence of the Skyros wall lizard Podarcis gaigeae: a combined role for local selection and genetic drift on color morph frequency divergence? *BMC Evol Biol* **10**, 15. (doi:10.1186/1471-2148-10-269).
17. Webb G.F., Blaser M.J. 2002 Dynamics of bacterial phenotype selection in a colonized host. *Proc Natl Acad Sci U S A* **99**(5), 3135-3140. (doi:10.1073/pnas.042685799).
18. Forsman A., Ahnesjo J., Caesar S., Karlsson M. 2008 A model of ecological and evolutionary consequences of color polymorphism. *Ecology* **89**(1), 34-40. (doi:10.1890/07-0572.1).
19. Wennersten L., Forsman A. 2012 Population-level consequences of polymorphism, plasticity and randomized phenotype switching: a review of predictions. *Biological Reviews* **87**(3), 756-767. (doi:10.1111/j.1469-185X.2012.00231.x).

20. Hughes A.R., Inouye B.D., Johnson M.T.J., Underwood N., Vellend M. 2008 Ecological consequences of genetic diversity. *Ecology Letters* **11**(6), 609-623. (doi:10.1111/j.1461-0248.2008.01179.x).
21. Summers K., Cronin T.W., Kennedy T. 2003 Variation in spectral reflectance among populations of Dendrobates pumilio, the strawberry poison frog, in the Bocas del Toro Archipelago, Panama. *J Biogeogr* **30**(1), 35-53. (doi:10.1046/j.1365-2699.2003.00795.x).
22. Brusa O., Bellati A., Meuche I., Mundy N.I., Prohl H. 2013 Divergent evolution in the polymorphic granular poison-dart frog, Oophaga granulifera: genetics, coloration, advertisement calls and morphology. *J Biogeogr* **40**(2), 394-408. (doi:10.1111/j.1365-2699.2012.02786.x).
23. Amezquita A., Castro L., Arias M., Gonzalez M., Esquivel C. 2013 Field but not lab paradigms support generalisation by predators of aposematic polymorphic prey: the Oophaga histrionica complex. *Evol Ecol* **27**(4), 769-782. (doi:10.1007/s10682-013-9635-1).
24. Ebersbach J., Posso-Terranova A., Bogdanowicz S., Gomez-Diaz M., Garcia-Gonzalez M.X., Bolivar-Garcia W., Andres J. 2020 Complex patterns of differentiation and gene flow underly the divergence of aposematic phenotypes in Oophaga poison frogs. *Mol Ecol* **29**(11), 1944-1956. (doi:10.1111/mec.15360).
25. Richards-Zawacki C.L., Wang I.J., Summers K. 2012 Mate choice and the genetic basis for colour variation in a polymorphic dart frog: inferences from a wild pedigree. *Mol Ecol* **21**(15), 3879-3892. (doi:10.1111/j.1365-294X.2012.05644.x).
26. McEwen B.L., Kinley I., Anderson H.M., Pruitt J.N., Yeager J., Barnett J.B. 2023 Batesians mimics are more detectable than their model in aerial and terrestrial view in a poison frog complex. *The American Naturalist (in Press)* **201**(2). (doi:doi/10.1086/722559).
27. Cummings M.E., Crothers L.R. 2013 Interacting selection diversifies warning signals in a polytypic frog: an examination with the strawberry poison frog. *Evol Ecol* **27**(4), 693-710. (doi:10.1007/s10682-013-9648-9).
28. Saporito R.A., Zuercher R., Roberts M., Gerow K.G., Donnelly M.A. 2007 Experimental evidence for aposematism in the dendrobatid poison frog Oophaga pumilio. *Copeia* (4), 1006-1011. (doi:10.1643/0045-8511(2007)7[1006:Eefait]2.0.Co;2).
29. Hegna R.H., Saporito R.A., Donnelly M.A. 2013 Not all colors are equal: predation and color polytypism in the aposematic poison frog Oophaga pumilio. *Evol Ecol* **27**(5), 831-845. (doi:10.1007/s10682-012-9605-z).
30. Richards-Zawacki C.L., Yeager J., Bart H.P.S. 2013 No evidence for differential survival or predation between sympatric color morphs of an aposematic poison frog. *Evol Ecol* **27**(4), 783-795. (doi:10.1007/s10682-013-9636-0).
31. Dreher C.E., Cummings M.E., Prohl H. 2015 An Analysis of Predator Selection to Affect Aposematic Coloration in a Poison Frog Species. *PLoS One* **10**(6), 18. (doi:10.1371/journal.pone.0130571).
32. Yeager J. 2015 Causes and consequences of warning color variation in a polytypic poison frog, Tulane University.
33. Willink B., Bolanos F., Prohl H. 2014 Conspicuous displays in cryptic males of a polytypic poison-dart frog. *Behavioral Ecology and Sociobiology* **68**(2), 249-261. (doi:10.1007/s00265-013-1640-4).
34. Summers K., Symula R., Clough M., Cronin T. 1999 Visual mate choice in poison frogs. *Proceedings of the Royal Society B-Biological Sciences* **266**(1434), 2141-2145. (doi:10.1098/rspb.1999.0900).
35. Reynolds R.G., Fitzpatrick B.M. 2007 Assortative mating in poison-dart frogs based on an ecologically important trait. *Evolution* **61**(9), 2253-2259. (doi:10.1111/j.1558-5646.2007.00174.x).
36. Tazzyman S.J., Iwasa Y. 2010 Sexual selection can increase the effect of random genetic drift - A quantitative genetic model of polymorphism in Oophaga pumilio, the strawberry poison-dart frog. *Evolution* **64**(6), 1719-1728. (doi:10.1111/j.1558-5646.2009.00923.x).
37. Fear K.K., Price T. 1998 The adaptive surface in ecology. *Oikos* **82**(3), 440-448. (doi:10.2307/3546365).
38. Osorio D., Miklosi A., Gonda Z. 1999 Visual ecology and perception of coloration patterns by domestic chicks. *Evol Ecol* **13**(7-8), 673-689. (doi:10.1023/a:1011059715610).
39. Jordan R., Kinderlehrer D., Otto F. 1997 Free energy and the Fokker-Planck equation. *Physica D* **107**(2-4), 265-271. (doi:10.1016/s0167-2789(97)00093-6).

40. Jordan R., Kinderlehrer D., Otto F. 1998 The variational formulation of the Fokker-Planck equation. *Siam Journal on Mathematical Analysis* **29**(1), 1-17. (doi:10.1137/s0036141096303359).
41. Brooks O.L., James J.J., Saporito R.A. 2023 Maternal chemical defenses predict offspring defenses in a dendrobatid poison frog. *Oecologia (in Press)*.
42. Summers K., Speed M.P., Blount J.D., Stuckert A.M.M. 2015 Are aposematic signals honest? A review. *J Evol Biol* **28**(9), 1583-1599. (doi:10.1111/jeb.12676).
43. Wolde-Kidan A., Herrmann A., Prause A., Gradzielski M., Haag R., Block S., Netz R.R. 2021 Particle Diffusivity and Free-Energy Profiles in Hydrogels from Time-Resolved Penetration Data. *Biophys J* **120**(3), 463-475. (doi:10.1016/j.bpj.2020.12.020).
44. Schulz R., Yamamoto K., Klossek A., Flesch R., Honzke S., Rancan F., Vogt A., Blume-Peytavi U., Hedtrich S., Schafer-Korting M., et al. 2017 Data-based modeling of drug penetration relates human skin barrier function to the interplay of diffusivity and free-energy profiles. *Proc Natl Acad Sci U S A* **114**(14), 3631-3636. (doi:10.1073/pnas.1620636114).
45. Grima R., Newman T.J. 2004 Accurate discretization of advection-diffusion equations. *Physical Review E* **70**(3). (doi:10.1103/PhysRevE.70.036703).
46. Akre K.L., Johnsen S. 2014 Psychophysics and the evolution of behavior. *Trends Ecol Evol* **29**(5), 291-300. (doi:10.1016/j.tree.2014.03.007).
47. MATLAB. 2019 *MATLAB and Statistics Toolbox Release 2019b, 9.7.0.1190202 (R2019b)*. Natick, Massachusetts, The MathWorks Inc.
48. Van Rossum G., Drake F.L. 2009 *Python 3 Reference Manual*. Scotts Valley, CA, CreateSpace.
49. Yeager J., Barnett J.B. 2022 Continuous Variation in an Aposematic Pattern Affects Background Contrast, but Is Not Associated With Differences in Microhabitat Use. *Frontiers in Ecology and Evolution* **10**, 10. (doi:10.3389/fevo.2022.803996).
50. Maan M.E., Seehausen O. 2011 Ecology, sexual selection and speciation. *Ecology Letters* **14**(6), 591-602. (doi:10.1111/j.1461-0248.2011.01606.x).
51. Blount J.D., Speed M.P., Ruxton G.D., Stephens P.A. 2009 Warning displays may function as honest signals of toxicity. *Proceedings of the Royal Society B-Biological Sciences* **276**(1658), 871-877. (doi:10.1098/rspb.2008.1407).
52. Kemp D.J., Reznick D.N., Grether G.F., Endler J.A. 2009 Predicting the direction of ornament evolution in Trinidadian guppies (Poecilia reticulata). *Proceedings of the Royal Society B-Biological Sciences* **276**(1677), 4335-4343. (doi:10.1098/rspb.2009.1226).
53. Parker G.A., Partridge L. 1998 Sexual conflict and speciation. *Philos Trans R Soc B-Biol Sci* **353**(1366), 261-274. (doi:10.1098/rstb.1998.0208).
54. Yang Y.S., Richards-Zawacki C.L. 2021 Male-male contest limits the expression of assortative mate preferences in a polymorphic poison frog. *Behavioral Ecology* **32**(1), 151-158. (doi:10.1093/beheco/araa114).
55. Lindstedt C., Lindstrom L., Mappes J. 2009 Thermoregulation constrains effective warning signal expression. *Evolution* **63**(2), 469-478. (doi:10.1111/j.1558-5646.2008.00561.x).
56. Nielsen M.E., Mappes J. 2020 Out in the open: behavior's effect on pedation risk and thermoregulation by aposematic caterpillars. *Behavioral Ecology* **31**(4), 1031-1039. (doi:10.1093/beheco/araa048).
57. Mori E., Mazza G., Lovari S. 2017 Sexual Dimorphism. In *Encyclopedia of Animal Cognition and Behavior* (ed. Vonk J.a.S., Todd), pp. 1--7. Cham, Springer International Publishing.
58. Rojas B., Endler J.A. 2013 Sexual dimorphism and intra-populational colour pattern variation in the aposematic frog Dendrobates tinctorius. *Evol Ecol* **27**(4), 739-753. (doi:10.1007/s10682-013-9640-4).
59. Bell R.C., Zamudio K.R. 2012 Sexual dichromatism in frogs: natural selection, sexual selection and unexpected diversity. *Proceedings of the Royal Society B-Biological Sciences* **279**(1748), 4687-4693. (doi:10.1098/rspb.2012.1609).
60. Langkilde T., Boronow K.E. 2012 Hot Boys Are Blue: Temperature-Dependent Color Change in Male Eastern Fence Lizards. *J Herpetol* **46**(4), 461-465. (doi:10.1670/11-292).
61. Smith K.R., Cadena V., Endler J.A., Porter W.P., Kearney M.R., Stuart-Fox D. 2016 Colour change on different body regions provides thermal and signalling advantages in bearded dragon lizards. *Proceedings of the Royal Society B-Biological Sciences* **283**(1832), 9. (doi:10.1098/rspb.2016.0626).

642 62. Lewis A.C., Rankin K.J., Pask A.J., Stuart-Fox D. 2017 Stress-induced changes in color
643 expression mediated by iridophores in a polymorphic lizard. *Ecol Evol* **7**(20), 8262-8272.
644 (doi:10.1002/ece3.3349).
645 63. Crothers L., Gering E., Cummings M. 2011 Aposematic signal variation predicts male-male
646 interactions in a polymorphic poison frog. *Evolution* **65**(2), 599-605. (doi:10.1111/j.1558-
647 5646.2010.01154.x).
648 64. Kikuchi D.W., Pfennig D.W. 2010 Predator Cognition Permits Imperfect Coral Snake Mimicry.
649 *American Naturalist* **176**(6), 830-834. (doi:10.1086/657041).
650 65. Kikuchi D.W., Pfennig D.W. 2013 Imperfect mimicry and the limits if natural selection *Q Rev Biol*
651 **88**(4), 297-315. (doi:10.1086/673758).
652 66. Katoh M., Tatsuta H., Tsuji K. 2017 Rapid evolution of a Batesian mimicry trait in a butterfly
653 responding to arrival of a new model. *Sci Rep* **7**, 7. (doi:10.1038/s41598-017-06376-9).
654